Carbohydrate Polymers 82 (2010) 370–375

Contents lists available at ScienceDirect

Carbohydrate Polymers

journal homepage: www.elsevier.com/locate/carbpol

FTIR and UV/vis as methods for evaluation of oxidative degradation of model paper: DFT approach for carbonyl vibrations

T. Łojewski[a,*], P. Miśkowiec[a,*], M. Missori[b], A. Lubańska[c], L.M. Proniewicz[a], J. Łojewska[a]

[a] Faculty of Chemistry, Jagiellonian University, Ingardena 3, 30-060 Kraków, Poland
[b] Istituto dei Sistemi Complessi, Consiglio Nazionale delle Ricerche, Via del Fosso del Cavaliere 100, I-00133 Rome, Italy
[c] Institute of Catalysis and Surface Chemistry, Polish Academy of Sciences, Niezapominajek 8, 30-239 Kraków, Poland

ARTICLE INFO

Article history:
Received 17 December 2009
Received in revised form 19 April 2010
Accepted 26 April 2010
Available online 12 May 2010

Keywords:
Cellulose oxidative degradation
FTIR
UV/vis
DFT

ABSTRACT

The oxidative route of cellulose degradation during artificial ageing of paper in humid air (RH 59%, 90 °C) has been followed by FTIR and UV/vis spectroscopic methods providing a vibrational pattern of carbonyl groups and electronic transitions of chromophores, respectively. Conjugated ketonic groups with vibrational modes around 1610 cm^{-1} were correlated to the chromophores emerging in the range between 230 and 440 nm detected by UV/vis spectroscopy. The FTIR spectra of degraded cellulose were interpreted using quantum-chemical modelling based on the DFT method performed on the model molecule of cellopentose. Based on this carbonyl FTIR bands were assigned to specific vibrations. The UV/vis and FTIR correlations together with the theoretical charge distribution rationalized the possible mechanism of oxidative glycosidic bond cleavage.

1. Introduction

1.1. Motivations

The problem of cellulose degradation we have been dealing with concerns, generally speaking, archival papers in books, but it also appears in electric transformers where paper is used as an insulator. In both applications the overall degradation mechanisms are different because the paper type and storage conditions are different. However, what both processes have in common is the oxidation route in the degradation network.

In books, fast degradation affects mainly the paper produced between 1850 and 1990 which constitutes a vast majority (about 80%) of the libraries and archives collections. Had it not been for the technical revolution in the paper making industry that took place around the year 1850, paper would have remained the most stable media. In fact, both the use of ground wood and the addition of alum in a new technological process have given rise to its dramatic chemical destabilisation which is manifested by brittling and yellowing of paper. This kind of cellulose degradation is caused mostly by the acidic hydrolysis of glucopyranose rings but also by oxidation (Barański, 2002; Barański, Konieczna-Molenda, Łagan, & Proniewicz, 2003; Barański, Łagan, & Łojewski, 2006). Even though mass deacidification programmes have been launched to prevent fast degradation all over the world, more investigation into its mechanism is still needed. More the knowledge than the experience should serve the conservators in choosing the proper methods of treatment of archival paper. The number of mistakes, the most serious of which is paper lamination, talk by themselves and support the idea.

In electricity transformers, in spite of the harsh conditions it is exposed to (air, temperature below 100 °C), paper degrades slowly but inevitably loosing its mechanical properties to the stage when it disintegrates. At such conditions the degradation is caused mainly by oxidation (Ali, Emsley, Herman, & Heywood, 2001). The decision on the paper exchange is critical for the economic reasons because the transformers are parts of the energy transmitting systems. Thus the trustworthy methods of monitoring the paper condition seem to be of high importance for electric power industry. In the literature there are several attempts to approach the problem by various analytical methods made mainly by Emsley's group (Emsley, Heywood, Ali, & Eley, 1997; Emsley, Xiao, Heywood, & Ali, 2000a; Emsley, Xiao, Heywood, & Ali, 2000b; Heywood, Emsley, & Ali, 2000).

This study intends to contribute to the discussion on paper degradation and in particular to provide reliable spectroscopic tools for the assessment of the progress of cellulose oxidation. It seems that without understanding the mechanism of cellulose oxidation, and through this, the understanding of the spectra, the choice of the analytical method is not possible. For these reasons the chemical analyses of the degraded paper are aided with the consideration

* Corresponding author. Tel.: +48 12 6632040; fax: +48 12 6340515.
E-mail addresses: lojewski@chemia.uj.edu.pl (T. Łojewski), miskowie@chemia.uj.edu.pl (P. Miśkowiec).

0144-8617/$ – see front matter © 2010 Elsevier Ltd. All rights reserved.
doi:10.1016/j.carbpol.2010.04.087

on the mechanisms of cellulose degradation and the quantum-chemical modelling of the vibrational spectra (Density Functional Theory, DFT). Of particular interest for us are the carbonylic groups of various degrees of freedom that appear as products of paper ageing which can be followed both in FTIR and UV/vis spectra.

1.2. Cellulose degradation

For acidic papers at ambient conditions without excess of heat or light, oxidation proceeds slowly, while hydrolysis runs fast due to catalytic effect of hydronium cations. A typical trend is that in their initial stage the rates are higher than in the advanced ageing, which can be accounted for by the exploitation of those regions in cellulose which are accessible for substrates – the disordered amorphous phase and at the surface of cellulose fibrils (Kraessig, 1993). For hydrolysis, the fact is signified by the so-called level off degree of polymerization (LODP) (Calvini, Gorassini, & Merlani, 2008; Lai, 2000).

While the mechanism of acidic hydrolysis is rather known and well-settled in the literature (Barański, Łagan, & Łojewski, 2005; Mosini, Calvini, Mattogno, & Righini, 1990; Zou, Uesaka, & Gurnagul, 1996), oxidation running through the radical mechanism initiated by active oxygen species ($O^{\bullet}$, $O_2^{\bullet}$) (Calvini & Gorassini, 2002; Strlič, Kolar, Kocar, & Rychly, 2005) is a complex process with a lot of possible reaction routes that can appear in cellulose and even more in paper material which constitutes chemically pre-processed multicomponent system. In fact, the most widespread knowledge of the oxidation mechanism concerns cellulose in water suspensions due to the interest of paper industry. Some information on selective oxidation in water solutions can be found in the exemplary references (Dupont, 1996; Fras et al., 2005; Mosini et al., 1990). The literature data on the oxidation mechanism during natural and accelerated ageing is much less abundant and studied mainly by Emsley, Strlič, Calvini groups and by us (Ali et al., 2001; Calvini et al., 2008; Calvini & Silveira, 2008; Emsley et al., 2000b; Kolar, 1997; Łojewska, Lubańska, Miśkowiec, Łojewski, & Proniewicz, 2006; Łojewska et al., 2007; Margutti, Conio, & Calvini, 2001; Strlič et al., 2005).

Oxidation of cellulose can be launched on the hydroxyl groups on C(2), C(3) and C(6) atoms in a glucopyranose unit, especially in acidic or neutral environment (Hon & Shiraishi, 2000). The oxidation propagates through consecutive and parallel paths (Łojewska, Lubańska, Łojewski, Miśkowiec, & Proniewicz, 2005; Łojewska et al., 2006) leading to the formation of various carbonyl groups. These are either single ketones on C(2) and C(3) transforming into conjugated diketones in the next oxidation step or aldehydes ending as carboxyls on C(6) (Łojewska, Lubańska et al., 2005; Łojewska et al., 2006; Łojewska, Miśkowiec, Łojewski, & Proniewicz, 2005). Oxygen or its active forms carried by water molecules may also attack directly C(1) atom involved in the glycosidic bond, leading to its cleavage.

Indubitably hydrolysis and oxidation are tangled together. What is known is that they exert a catalytic effect on one another (Łojewska, Lubańska et al., 2005). The formation of carboxylic groups upon oxidation promotes hydrolysis and conversely, hydrolysis provides new reducing end groups for oxidation. Additionally, the appearance of water as oxidation side product provides the substrate for hydrolysis. Water can also be regarded as the transporting agent for both protons and active oxygen for hydrolysis and oxidation, respectively.

2. Experimental

For the study, model paper samples (P1, 99.5% cellulose) obtained from TNO, the Netherlands, and described in Łojewska, Lubańska et al. (2005) and Łojewska, Miśkowiec et al. (2005) were used. The paper comes from softwood sulphite bleached pulp and has been described as slightly acidic (pH 6.3) and containing inorganic ingredients measured as ash constant (0.45%) and traces of lignin. As it originates from softwood we may expect hemicellulose in its composition. They were artificially aged in a climatic chamber under 59% of relative humidity (RH) in the air at 90 °C temperature for various periods (0–46 days). Then the conditioned samples were subjected to further analyses.

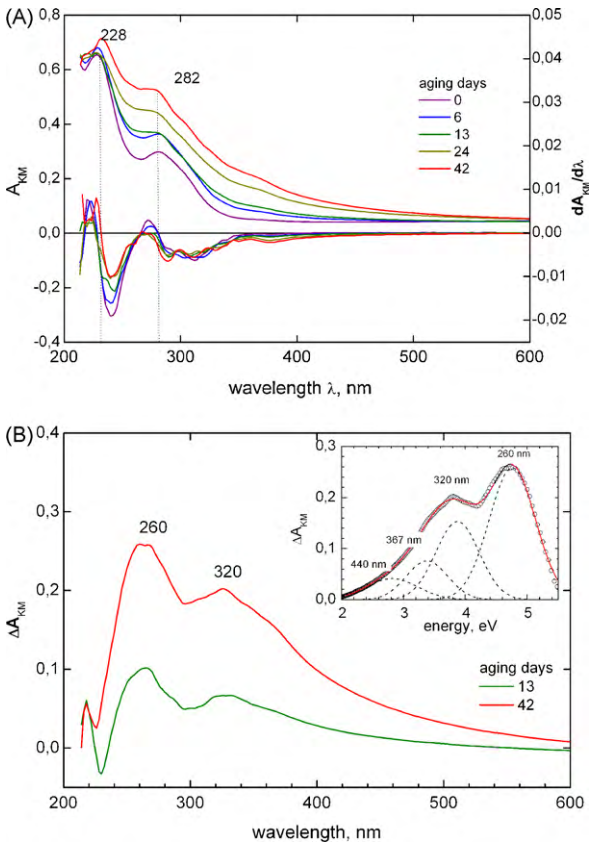

Fig. 1. (A) Reflectance UV/vis spectra of P1 paper samples aged for various periods in humid air (RH 59%) at 90 °C transformed to pseudo-absorbance A_{KM} by Kubelka–Munk function (left axis, upper curves), and its first derivative (right axis, lower curves). (B) Difference spectra of samples aged for 42 and 13 days subtracted with the one of the unaged sample. Inset, the Gaussian fit of the difference spectrum of sample aged 42 days.

UV/vis diffuse reflectance spectra were measured at room temperature and at 50% RH conditions by using a Jasco V-570 spectrophotometer equipped with a $BaSO_4$ coated integrating sphere and PbS detector, and normalized to a Spectralon diffuse reflectance reference standard (factory calibrated). The spectra resolution was set to 5 nm while data were pitched every 2 nm. The UV/vis spectra of the samples aged for various periods are shown as pseudo-absorbance calculated from reflectance through the Kubelka–Munk transformation (Fig. 1, panel A) (Kubelka, 1948).

The FTIR spectra were collected on Excalibur 3000 Digilab spectrometer with DTGS detector at an optical resolution of 2 cm^{-1} in a measuring cuvette operating in a vacuum at 90 °C. The measuring time was short enough to prevent any significant additional aging of the samples. It has been proved before (Łojewska, Lubańska et al., 2005; Łojewska et al., 2006) that under such conditions water desorbs from paper samples leaving the spectra range of our interest free from water bending vibrations around 1640 cm^{-1}. The FTIR were normalized using an internal standard method (integral of CH band between 2800 and 3000 cm^{-1}). The details concerning the apparatus and procedures can be found in Łojewska, Lubańska et al. (2005).

3. Calculations

The calculations were performed for a cellopentose molecule (Łojewska et al., 2006) to avoid prolonged procedures involving the quantum statistics usually necessary for polymer molecules. Cellopentose has been shown to be the shortest oligomer built of the β-D-glucopyranose monomer whose FTIR spectra practically do not differ from the spectra of cellulose polymer (Michell & Higgins, 2002; Sekkal, Dincq, Legrand, & Huvenne, 1995). The calculations were executed using the GAUSSIAN 03 package (Frisch et al., 2004) by the DFT method with a basis set 6-31G using B3LYP hybrid functional. Prior to frequency simulations the geometry of model molecules and their oxidized derivatives was optimized for the lowest energy conformations. Optimum geometries and harmonic frequencies were determined on the SGI 2800 computer. The spectra were optimized to reproduce the experimental spectra of cellulose. The frequencies were scaled according to the frequency calibration presented in Łojewska et al. (2006) and the literature data (Johnson, 2006; Scott & Radom, 1996). For the range where –CO vibrations occur (1500–1900 cm^{-1}) the scaling factor was found to be 0.9614. The calculated intensities of the calculated spectra were transformed into absorbance values. The charges distribution was calculated according to the Atomic Polar Tensor (APT) method.

4. Results and discussion

The first issue to be discussed is what kind of information concerning degradation is provided by UV/vis and FTIR methods. Without question, the FTIR spectroscopy is able to grasp the vibrations of carbonyl groups in the range where stretching vibration modes appear (1800–1500 cm^{-1}). These all are the products of both oxidation and hydrolysis. At humid air atmosphere and at elevated temperature used for artificial ageing, oxidation accelerates and contributes significantly to the overall degradation process (Barański, 2002). The effect of hydrolysis in FTIR spectra cannot, however, be huge. The population of reducing end groups (–CHO), which are the products of hydrolysis of glycoside bonds measurable by FTIR is low in comparison with the oxidation products simply because the number of glycosidic bonds is less than the number of –C–OH groups available for oxidation in the accessible regions of cellulose at least at the low advanced oxidation stage of cellulose. Even though the population of terminal rings grows upon hydrolysis and thus grows the number of aldehydic groups in their open forms, it always remains much lower than the prevailing majority of oxidation products on the whole polymer. On the other hand, the quantitative interpretation of the vibrational modes of glycosidic bonds is practically impossible in FTIR because the characteristic hemiacetal vibration emerging at 897 cm^{-1} (Hon & Shiraishi, 2000) is not intense and it is masked by other associated vibrations of glucopyranose ring which prevail around 1000 cm^{-1} in the cellulose spectrum. In this way FTIR can be treated more as a tool to follow oxidative degradation of cellulose rather than the hydrolytic one. The information provided by UV/vis is limited to those carbonyls which form conjugated double bond system, the most active for electronic transitions (Silverstein, Bassler, & Morrill, 1974). Thus using both methods we shall be able to distinguish between the oxidation pathways towards various carbonyls.

4.1. Experimental spectra

4.1.1. UV/vis

UV/vis pseudo-absorbance of the unaged sample shows two distinct maxima at 228 and 282 nm. Upon ageing, while these two maxima grow to remain evident, the overall intensity of pseudo-absorbance in the UV/vis increases, and a new shoulder around 360 nm emerges (Fig. 1A). The evolution of the spectral features can be distinguished in a more convenient way in the first derivative spectra shown in Fig. 1B. The first derivatives reach 0 values in correspondence of the 228 nm maxima only for less aged samples (0 and 6 ageing days). The maxima of the first derivatives around 242 nm decreases continuously with increasing degradation, indicating a decreasing slope of the spectra in this spectral region. On the contrary the first derivatives increase minutely but continuously at around 380 nm with aging time. This kind representation of the time trends of the spectra does not necessarily shows the evolution of new bands but simply the features of the absorbance function. The increase of the absorbance maxima and the inflection points can be a result of the development of the sub bands hidden in the broad pattern of electronic transitions visible on the spectra. To recognize the new bands evolving with aging time, difference spectra are presented in Fig. 1B (the spectra of samples aged for 42 and 13 days are subtracted with the spectrum of the unaged sample). Two broad asymmetric bands at around 260 and 320 nm are different than on the original spectra. The difference spectrum of the sample aged 42 days was fitted using Gaussian peaks in the spectral energy range (see inset of Fig. 1B). Best fitting was achieved using 4 Gaussian functions with maxima at 260 nm, 320 nm, 367 nm and 440 nm corresponding to full-width-at-half-height (FWHH) values at 48, 45, 43 and 54 nm, respectively.

High intensities of the bands evolved in the UV range suggest that the species showing them have conjugated double bonds since the single double bonds are not equally active in UV/vis (Silverstein et al., 1974). They may arise from two possible electronic excitations $n \rightarrow \pi^*$ and $\pi \rightarrow \pi^*$. However, since there are more than two bands evolving in this range of the spectra of the aged samples according to the results of the fitting of the Gaussian functions there are most evidently more than just one degradation products with a conjugated double bond system. These may arise from both conjugated ketonic groups and their enolic forms.

4.1.2. FTIR

Together with the development of the bands representing electronic transitions a broad band at around 1610 cm^{-1} increases with aging time in the vibrational spectra collected for the same set of the samples (Fig. 2A). Since, the bands do not seem to show pure vibrations, following the features delivered by the first derivative, they were fitted with multi-Gaussian functions. This is shown by an exemplary fitting of the spectrum corresponding to the sample aged for 13 days (Fig. 2B). An optimum correlation was achieved for 8 Gaussian functions in the range 1500–1850 cm^{-1}, except for the sample aged for 46 days whose spectra were even more complex and needed 10 functions. The calculated wavenumbers of the maxima for a given sample together with the mean frequencies of the particular bands and their standard deviations obtained from fitting are included in Table 1. The FWHH of the fitted Gaussians are rather high, however, due to the fact that degradation products develop principally in the amorphous cellulose phase, from their nature, the bands cannot reflect pure vibrational modes as has also been discussed in Buslov, Nikonenko, Sushko, and Zhbankov (2000) and Buslov, Nikonenko, Sushko, and Zhbankov (2001). Additionally, due to the rearrangement of the hydrogen bond network and the changes in the effective potential energy resulting from the chemical environment modifications varying with ageing time, the positions of the maxima of particular chemical ensembles may shift towards slightly lower or higher wavenumber giving as a result practically inseparable band broadening and shift of the positions of the maxima. For this reason also the accuracy of the fitting cannot be very high because of the several local minima of the residues function in the optimized parameter space. Thus the optimized wavenumbers of the maxima of the less developed bands are only

Table 1
Frequencies of carbonyl vibrations obtained from the fitting of Gaussian functions to the degraded cellulose spectra in the range 1500–1900 cm^{-1}.

Ageing time (days)	Band wavenumber, ν (cm^{-1})									
	1	2	3	4	5	6	7	8	9	10
0	1542		1608	1669	1685	1704	1739		1791	1833
6	1545		1606	1649	1677	1704	1731		1790	1844
13	1559		1604	1633	1676	1710	1751		1808	1842
25	1544		1606	1639	1683	1722	1755		1801	1838
46	1551	1577	1608	1659	1691	1700	1736	1783	1813	1836
Mean	1548		1606	1650	1682	1708	1742		1801	1839
Std. dev.	6		1	13	5	8	9		9	4

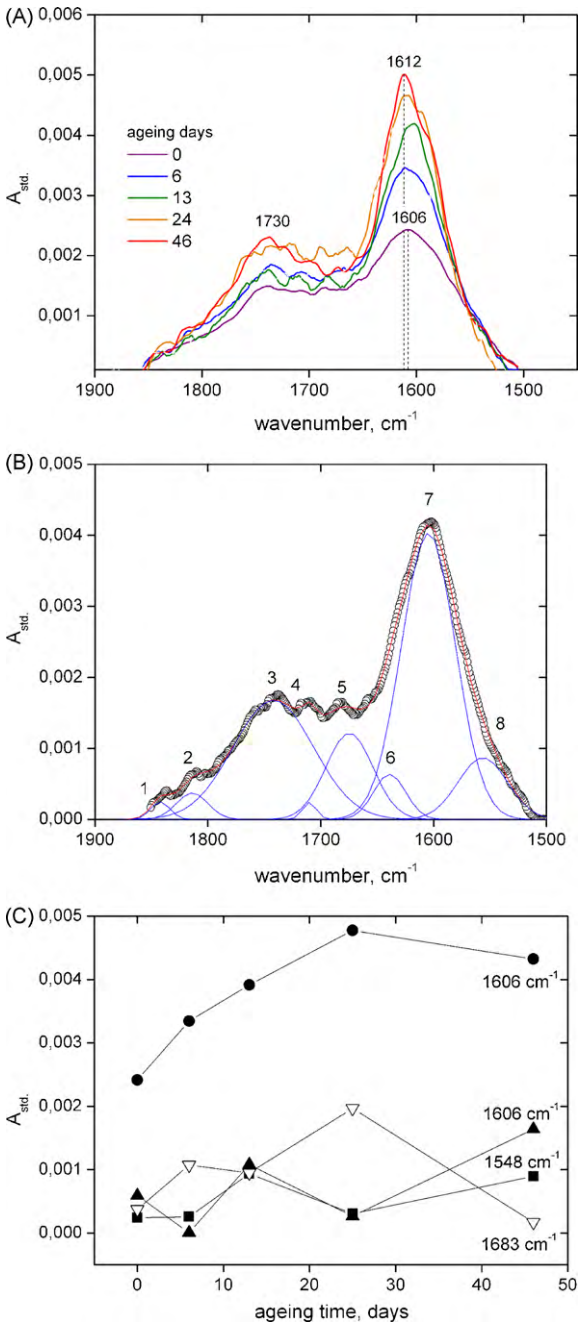

Fig. 2. (A) FTIR spectra of P1 samples aged for various periods in humid air (RH 59%) at 90 °C recalculated to standardized absorbance A_{std}. (B) Exemplary fitting of Gaussian functions to the spectrum for the sample aged for 13 days. (C) Ageing time dependence on the intensity of the fitted bands.

approximate with a high scatter as shown in Table 1. However, the most apparent maximum at around $1606 \pm 1\ cm^{-1}$ whose growing intensity is presented in Fig. 2C has a fairly fixed position. The collapse of this growing tendency observed at 46 days can be due to the appearance of another oxidation product in a series giving a lower frequency band at $1577\ cm^{-1}$ or the exploitation of the amorphous cellulose phase. The intensities of the other higher frequency bands do not show clear growing tendencies for the reason given above (Fig. 2C).

At this stage of the spectra analysis the band assignment to specific vibrations would be far too speculative if not aided with the additional independent methods.

4.2. Theoretical spectra

Quantum-chemical calculations of the spectra shed some more light on the interpretation of the results and in this way the possible degradation products of cellulose. They were performed according to the procedure described in the previous chapter and in more detail in our former article (Łojewska et al., 2006). The calculated frequencies should not be treated absolutely even though they were scaled, since paper is a much more complex system than the model molecule of cellopentose used for the spectra simulations. The relative frequency values may, however, be useful to increase our understanding of the degradation process taking place in paper material.

The theoretical values of the frequencies of the carbonylic groups at various positions within a glucopyranose ring (carbon atom number) and on various rings (ring number) of the model molecule of cellopentose are presented in Table 2. The frequency of a particular carbonylic group is fairly stable giving a standard deviation less than $9\ cm^{-1}$. The exception is the low intensity band with the mean value of $1681 \pm 23\ cm^{-1}$ originating from the antisymmetric vibrations of conjugated diketones. In contrast, the symmetric vibrations of the conjugated ketones of high intensity appears at $1643 \pm 4\ cm^{-1}$. It is also worth pointing out that for carbonylic groups the highest frequencies occur for terminal carbonylic groups or, more precisely, on the first or the last ring, but their contribution to the overall spectra is expected to be rather low due to their low population in the polymer.

The conjugated ketones together with their enolic tautomeric forms are assumed by us to appear as the products of moderate oxidation of cellulose. While the diketones were observed by other authors at similar frequencies (Calvini & Gorassini, 2002; Mosini et al., 1990), there is no strong evidence in our experimental results for the formation of enols on glucopyranose rings (Łojewska et al., 2006). The exemplary simulation of the vibrations of the enolic group on C(3) atom on the 3rd ring in cellopentose molecule is presented in Table 3 together with the results obtained for single ketones and conjugated ketones on the same ring. According to the calculations the vibration of C=C–OH group should emerge at higher frequency than the ketones $1752\ cm^{-1}$ (scaling factor 0.9614). This is in accordance with the literature experimental data

Table 2
Frequencies of carbonyl vibrations calculated by DFT for various positions on cellopentose oligomer (ring numbers from "tail" to "head") and various positions on a given ring (C atom number). Frequencies scaled by 0.9614 factor.

Ring number	Carbon atom number in glucopyranose ring						
	C(1)	C(2)	C(3)	C(4)	C(2,3)		C(6)
1	–	1674	1665	1643	1641	1680	1645
2	–	1675	1651	–	1640	1725	1662
3	–	1675	1653	–	1640	1664	1672
4	–	1667	1658	–	1643	1679	1657
5	1722	1672	1659	–	1650	1658	1655
Mean		1673	1657		1643	1681	1658
Std. dev.		3	5		4	23	9

Table 3
Comparison of the frequencies of ketonic and enolic vibrations found by DFT method for the ring 3. Frequencies scaled by 0.9614 factor.

Carbonyls	Atom number	Wavenumber, ν (cm^{-1})	
Ketone	C(2)	1675	–
Ketone	C(3)	1651	–
Conjugated ketone	C(2,3)	1640	1672
Enol	C(3)	1752	–

(Ali et al., 2001) where the enols are said to emerge at around 1680 cm^{-1} in the FTIR spectrum which is by around 70 cm^{-1} higher than diketones found by us. In the Raman spectrum of the degraded paper discussed in our previous paper the weak bands evolving near 1680 cm^{-1} may be assigned to the vibrations of C=C groups (Łojewska et al., 2007). Additional but indirect evidence for the formation of enolic groups together with diketones on the degradated cellulose comes from the analysis of the UV/vis as mentioned above.

Another view of degradation phenomena can be achieved from the theoretical study of the charge distribution on the atoms of the oxidized cellopentose molecule. An example of the calculations is presented in Fig. 3. No matter what kind of cellopentose molecule we consider in terms of the position of conjugated ketonic groups and of the extent of oxidation, the highest negative charge is always localized on the oxygen atoms in the nearest glycosidic bond in the vicinity of ketones. Suppose conjugated ketones formed on one of the glucopyranose rings and the π bond in C(3)=O group (or C(2)=O) shifted towards the ring forming the enolic group C(4)=C(3)–OH, the electrons should further be shifted towards electronegative oxygen – the most negatively charged oxygen atom in the glycosidic bond. As a result, this should set out the glycosidic bond cleavage. This effect should also be attenuated by the change of the glucopyranose ring conformation due to oxidation from the chair ring to the partly flat ring with ketones.

There is a striking similarity in the shape of the experimental spectra of degraded (oxidized) samples and the theoretical spectrum of the oxidized cellopentose in which all C(2), C(3) atoms as well as C(1) and C(4) atoms on the first and the last ring were oxidized to ketones giving altogether 12 carbonylic groups denoted as 12CO (Fig. 4A). In order to match both spectra the frequencies of the calculated spectrum should be shifted by 26 cm^{-1}. This transformation, however slightly risky, may be treated as an additional correction giving new scaling factor 0.9461 for the discussed spectrum range. The scaling factor may reflect the transition from the model cellopentose molecule to the cellulose in paper. The coincidence in both spectra shape at a lower frequency range (<1700 cm^{-1}) supports the hypothesis of the moderate oxidation (towards ketones rather than carboxyls) that takes place under the ageing conditions used, additionally supported by the UV/vis results. A comparison of the spectra obtained for the other boundary situations when all C(6) atoms were transferred into both aldehydic (5CHO) or to carboxylic groups (5COOH) and finally

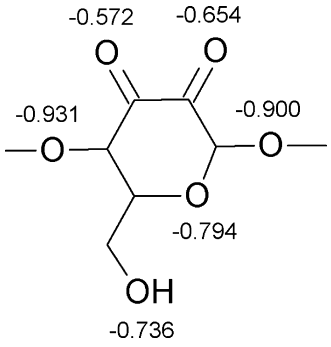

Fig. 3. Charge distribution on oxygen atoms on the 3rd ring of the cellopentose molecule oxidized to conjugated ketones C(2,3) calculated according to the APT method.

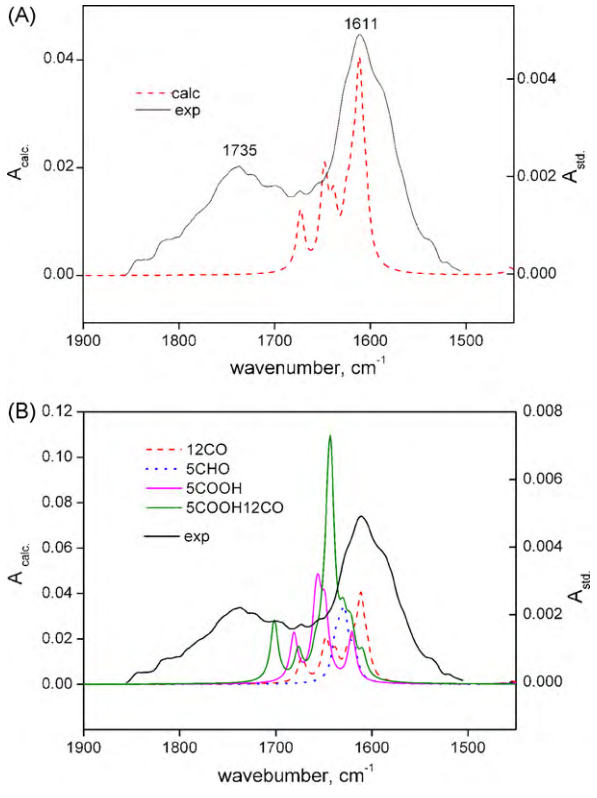

Fig. 4. (A) Comparison of theoretical spectrum of cellopentose oxidized to ketones on each glucopyranose ring (12CO) with experimental FTIR spectrum obtained for P1 sample aged for 46 days. (B) Comparison of theoretical FTIR spectra for various oxidation stages of cellopentose: 12CO, conjugated ketones on each ring plus ketones on C(4) and aldehydes C(1) atoms on the tail (1) and the head (5) ring, respectively; 5CHO, aldehydes on C(6) atom on each ring; 5COOH, carboxyls on C(6) atom on each ring. Calculated frequencies scaled by 0.9461 factor.

the whole cellopentose was oxidized (5COOH12CO) is presented in Fig. 4B (scaled by 0.9461). The general trend is that the maximum shifts towards higher frequencies moving from ketones to aldehydes and carboxyls and finally to fully oxidized cellopentose. The contribution of the vibrations of aldehydes and carboxyls from more oxidized polymer becomes visible for more degraded sample (ageing time 46 days) where the higher frequency bands start to expand above 1700 cm^{-1}. The results of the calculations suggest that carboxylic groups' vibrations can appear at higher frequencies than the ranges typically given in the frequency charts for the organic compounds.

5. Conclusions

- FTIR and UV/vis were shown to be partly complementary methods to follow oxidative degradation of cellulose.
- Carbonyl vibrational modes (1606 cm^{-1}) in FTIR spectra were correlated with electronic excitations in chromophores UV/vis spectra (260 and 320 nm).
- Quantum mechanic calculations using the DFT method supported bands assignment to conjugated ketones in FTIR spectra on partly oxidized cellulose. They show the possibility of formation of enolic groups on degraded cellulose with which ketonic group may constitute another chromophore on degraded cellulose chain. Also, they indicate the high frequency vibrations (above 1700 cm^{-1}) of carboxylic groups on more advanced stages of cellulose degradation.
- The experimental and theoretical results support the hypothesis of the moderate oxidation of cellulose at humid atmosphere (RH 59%) at 90 °C leading mostly to conjugated diketones. Further less intense oxidation was shown to proceed through aldehydes to carboxyls at more advanced state of degradation.
- Based on the experimental and theoretical results the hypothesis of the oxidative glycosidic bond cleavage was put forward. It assumes that the change in the hybridization of the carbon C(2) and C(3) atoms (from sp^3 to sp^2) together with the charge transfer from ketonic to enolic groups gives rise to the glycosidic bond cleavage. The idea is supported by the charge distribution calculations on the oxidized cellopentose.

Acknowledgments

The authors thank the Academic Computer Centre Cyfronet in Krakow (Poland) for granted computer time (grant no. MNiI/SGI2800/UJ/020/2004). The study was partly supported by the grant SPB K/PMN/000018 from Polish Ministra of Science and Higher Education.

References

Ali, M., Emsley, A. M., Herman, H., & Heywood, R. J. (2001). Spectroscopic studies of the ageing of cellulosic paper. *Polymer*, *42*, 2893–2900.
Barański, A., Konieczna-Molenda, A., Łagan, J. M., & Proniewicz, L. M. (2003). Catastrophic room-temperature degradation of cellulose. *Restaurator*, *4*, 36–45.
Barański, A. (2002). Ageing kinetics of cellulose and paper. *Restaurator*, *23*, 77–88.
Barański, A., Łagan, J. M., & Łojewski, T. (2005). Acid catalysed degradation. In M. Strlič (Ed.), *Aging and stabilisation of paper* (pp. 93–109) (Ljubljana).
Barański, A., Łagan, J. M., & Łojewski, T. (2006). The concept of mixed-control mechanisms and its applicability to paper degradation studies. *e-Preservation Science*, *3*, 1–4.
Buslov, D. K., Nikonenko, N. A., Sushko, N. I., & Zhbankov, R. G. (2000). Resolution enhancement in IR spectra of carbohydrates by the deconvolution method and comparison of the results with low-temperature spectra. *Applied Spectroscopy*, *54*, 1651–1658.
Buslov, D. K., Nikonenko, N. A., Sushko, N. I., & Zhbankov, R. G. (2001). Profile shape of absorption spectra in the IR spectra of carbohydrates. *Journal of Applied Spectroscopy*, *68*, 917–923.
Calvini, P., & Gorassini, A. (2002). FTIR—deconvolution spectra of paper documents. *Restaurator*, *23*, 48–66.
Calvini, P., Gorassini, A., & Merlani, A. L. (2008). On the kinetics of cellulose degradation: Looking beyond the pseudo zero order rate equation. *Cellulose*, *15*, 193–203.
Calvini, P., & Silveira, M. (2008). FTIR analysis of naturally aged $FeCl_3$ and $CuCl_2$-doped cellulose papers. *e-Preservation Science*, *5*, 1–8.
Dupont, A. L. (1996). Degradation of cellulose at the wet/dry interface. II. An approach to the identification of the oxidation compounds. *Restaurator*, *17*, 145–164.
Emsley, A. M., Heywood, R. J., Ali, M., & Eley, C. M. (1997). On the kinetics of degradation of cellulose. *Cellulose*, *4*, 1–5.
Emsley, A. M., Xiao, X., Heywood, R. J., & Ali, M. (2000a). Degradation of cellulosic insulation in power transformers. Part 2: Formation of furan products in insulating oil. *IEE Proceedings: Science, Measurement and Technology*, *147*, 110–114.
Emsley, A. M., Xiao, X., Heywood, R. J., & Ali, M. (2000b). Degradation of cellulosic insulation in power transformers. Part 3: Effects of oxygen and water on ageing in oil. *IEE Proceedings: Science, Measurement and Technology*, *147*, 115–119.
Fras, L., Johansson, L. S., Stenius, P., Laine, L., Stana-Kleinschek, K., & Ribitsch, V. (2005). Analysis of the oxidation of cellulose fibres by titration and XPS. *Colloids and Surfaces A: Physicochemical and Engineering Aspects*, *260*, 101–108.
Frisch, M. J., Trucks, G. W., Schlegel, H. B., Scuseria, G. E., Robb, M. A., et al. (2004). *Gaussian 03, Revision C.02*. Wallingford, CT: Gaussian, Inc.
Heywood, R. J., Emsley, A. M., & Ali, M. (2000). Degradation of cellulosic insulation in power transformers. Part 1: Factors affecting the measurement of the average viscometric degree of polymerisation of new and aged electrical papers. *IEE Proceedings: Science, Measurement and Technology*, *147*, 86–90.
Hon, D. N., & Shiraishi, N. (2000). *Wood and cellulosic chemistry*. New York: Marcel Dekker.
Johnson, R. D., III. (2006). *NIST computational chemistry comparison and benchmark database*. National Institute of Standards and Technology.
Kolar, J. (1997). Mechanism of autooxidative degradation of cellulose. *Restaurator*, *18*, 163–176.
Kraessig, H. (1993). *Cellulose: Structure, accessibility, and reactivity*. Yverdon: Gordon and Breach Science., 376 pp.
Kubelka, P. (1948). New contributions to the optics of intensely light-scattering materials. Part I. *Journal of the Optical Society of America*, *38*, 448.
Lai, Y.-Z. (2000). Chemical degradation. In D. N. Hon, & N. Shiraishi (Eds.), *Wood and cellulosic chemistry*. New York: Marcel Dekker.
Łojewska, J., Lubańska, A., Łojewski, T., Miśkowiec, P., & Proniewicz, L. M. (2005). Kinetic approach to degradation of paper. In situ FTIR transmission studies on hydrolysis and oxidation. *e-Preservation Science*, *2*, 1–12.
Łojewska, J., Lubańska, A., Miśkowiec, P., Łojewski, T., & Proniewicz, L. M. (2006). FTIR in situ transmission studies on the kinetics of paper degradation via hydrolytic and oxidative reaction paths. *Applied Physics A: Materials Science & Processing*, *83*, 597–603.
Łojewska, J., Missori, M., Lubanska, A., Grimaldi, P., Zieba, K., et al. (2007). Carbonyl groups development on degraded cellulose. Correlation between spectroscopic and chemical results. *Applied Physics A: Materials Science & Processing*, *89*, 883–887.
Łojewska, J., Miśkowiec, P., Łojewski, T., & Proniewicz, L. M. (2005). Cellulose oxidative and hydrolytic degradation: In situ FTIR approach. *Polymer Degradation and Stability*, *88*, 512–520.
Margutti, S., Conio, G., & Calvini, P. E. P. (2001). Hydrolytic and oxidative degradation of paper. *Restaurator*, *22*, 67–83.
Michell, A. J., & Higgins, H. G. (2002). *Infrared spectroscopy in Australian forest products research*. Melbourne: CSIRO Forestry and Forest Products.
Mosini, V., Calvini, P., Mattogno, G., & Righini, G. (1990). Derivative infrared spectroscopy and electron spectroscopy for chemical analysis of ancient paper documents. *Cellulose Chemistry and Technology*, *24*, 263–272.
Scott, A. P., & Radom, L. (1996). Harmonic vibrational frequencies: An evaluation of Hartree–Fock, Moller–Plesset, quadratic configuration interaction, density functional theory, and semiempirical scale factors. *The Journal of Physical Chemistry*, *100*, 16502–16513.
Sekkal, M., Dincq, V., Legrand, P., & Huvenne, J. P. (1995). *Journal of Molecular Structure*, *349*, 349–352.
Silverstein, R., Bassler, G., & Morrill, T. C. e. (1974). *Spectrometric identification of organic compounds*. New York: John Wiley.
Strlič, M., Kolar, J., Kocar, D., & Rychly, J. (2005). Thermo-oxidative degradation. In *Aging and stabilisation of paper* (pp. 111–132 (Ljubljana)).
Zou, X., Uesaka, T., & Gurnagul, N. (1996). Prediction of paper permanence by accelerated aging. 2. Comparison of the predictions with natural aging results. *Cellulose*, *3*, 269–279.